CHAPTER 8: RESULTS

Current-Voltage Temperature characteristics of n-Ge (100) Schottky barrier diodes

8.1 Introduction

Metal-semiconductor (MS) contacts are the most widely used rectifying contacts in the electronic industry [1,2,3,4,5,6,7]. The performance and reliability of a Schottky diode is drastically influenced by the interface quality between the deposited metal and semiconductor surface [1,8,9]. It is often found that the current-voltage (*I-V*) characteristics of MS contacts usually deviate from the ideal thermionic emission (TE) current model [4,5,6,10,11,12]. The temperature dependence of barrier parameters of homogeneously doped Schottky contacts has been studied by several authors [13,14,15,16,17,18,19,20,21,22,23,24]. It was found that the barrier height (BH) extracted from *I-V* measurements using TE theory decreases and ideality factor increases with decreasing temperature. The standard TE theory fails to explain this result [19], as it expects the BH variation to be controlled only by the variation of band gap with temperature [13]. Schottky diodes (SDs) with low BH have found applications in devices operating at cryogenic temperatures, such as infrared detectors and sensors in thermal imaging [7,25,26,27]. Therefore, analysis of *I-V* characteristics of the Schottky barrier diodes (SBDs) at room temperature only does not give detailed information about their conduction process or the nature of barrier formation at the MS interface. The temperature dependence of the *I-V* characteristics allows us to understand different aspects of conduction mechanisms. Although, BH in Schottky contacts is likely to be a function of the atomic structure, and the atomic inhomogeneities at MS interface which are caused by grain boundaries, defects, multiple phases, etc. [28,29,30,31], additionally, there may be doping inhomogeneity at the MS interface and dopant clustering. Contaminants due to undesirable reaction products at the MS interface may act directly to introduce inhomogeneities [7] or they may simply promote inhomogeneity, through the generation of

defects [29,30,31,32,33]. There has been no report on the electrical transport characteristics of germanium (Ge) Schottky contacts at low temperatures. Therefore an attempt has been made to study the current transport characteristics of Pd-, Ni- and Au/n-Ge Schottky diodes in the temperature range 60-300 K. The temperature dependence of the BH and the ideality factor are discussed using TE theory.

8.2 Experimental procedures

SDs were fabricated on Sb-doped n-type Ge substrate with doping concentration of 2.5×10^{15} cm^{-3}. The substrates were sequentially degreased with organic solvents like trichloroethylene, acetone and methanol by ultrasonic agitation for 5 min in each stage followed by rinsing in deionised water. The native oxide on the surfaces was etched in a mixture of H_2O_2(30%):H_2O (1:5) for 1 min. After rinsing in deionised water the samples were blown dried using N_2. Immediately after cleaning the samples were inserted into a vacuum chamber where 100 nm thick AuSb (0.6%) was deposited by resistive evaporation as a back ohmic contact, followed by annealing at 350°C in Ar ambient for 10 min to minimize the ohmic contact's resistivity. Before Schottky contacts deposition, the samples were again chemically cleaned as described above. Palladium (Pd), gold (Au) and nickel (Ni) Schottky contacts were deposited onto Ge by vacuum resistive evaporation. These contacts were deposited under vacuum with a pressure below 10^{-6} Torr. The contacts were 0.6 mm in diameter and 30 nm thick. Following contact fabrication, current-voltage (*I-V*) measurements were performed in the temperature range 40-300 K.

8.3 Results and discussion

8.3.1 The current-voltage characteristics as a function of temperature

To understand whether or not a SD has an ideal diode behaviour, an analysis of its experimental *I-V* characteristics must be performed using the TE model [1]:

$$I(V) = I_0 \exp\left(\frac{qV}{nkT}\right)\left[1-\exp\left(-\frac{qV}{kT}\right)\right], \tag{8.1}$$

with

$$I_0 = A^* A T^2 \exp\left(-\frac{q\Phi_B}{kT}\right), \tag{8.2}$$

where I_0 is the saturation current derived from the straight line intercept of the ln(I) – V plot at $V = 0$, V is the forward bias voltage, T is the absolute temperature, q is the electronic charge, k is the Boltzmann constant, A is the effective diode area, A^* is the effective Richardson constant, and Φ_B the zero bias effective SBH. From Eq. (8.2), we have:

$$\Phi_B = \frac{kT}{q} \ln\left(\frac{A^* A T^2}{I_0}\right), \tag{8.3}$$

and n is the ideality factor, which can be obtained accurately from the slope of the linear part of a ln (I) versus V plot, assuming pure thermionic emission can be obtained from Eq. (8.1) as

$$n = \frac{q}{kT} \frac{dV}{d(InI)}, \tag{8.4}$$

which is equal to 1 for an ideal diode and usually has a value greater than unity.

Typical forward bias I-V characteristics of Ni-/, Pd-/ and Au/n-Ge (100) Schottky contacts measured in the temperature range 60-300 K are shown in Figs. 8.1 – 8.3, respectively. These curves indicate a very strong temperature dependence of the Schottky diodes. These characteristics deviate from ideality at low temperatures (60 – 220 K), which are due to the effect of other current transport processes like the generation-recombination of carriers in space charge region [8] and tunnelling of electrons through the barrier. At temperatures above 220 K, thermionic emission becomes the dominant process. The experimental values of Φ_B and n were determined from intercepts and slopes of the forward ln (I) *versus* V plot at each temperature using the TE theory, respectively. That is, Φ_B and n were evaluated from the upper part of the temperature-dependent forward-bias I-V characteristics from 40 to 220 K .

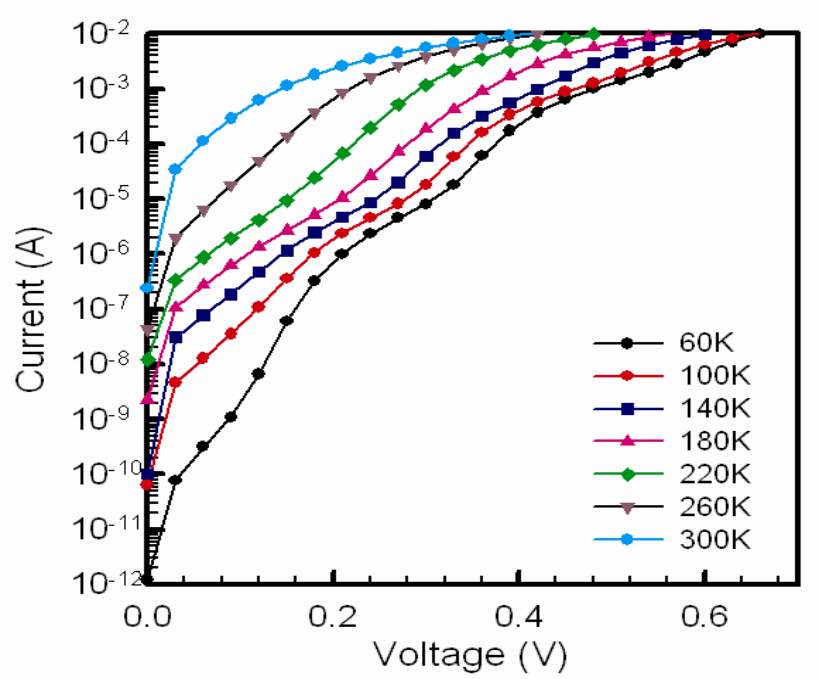

Fig. 8.1 *Experimental forward-bias current-voltage characteristics of a Ni/n-Ge (100) Schottky contact in the temperature range 60-300 K.*

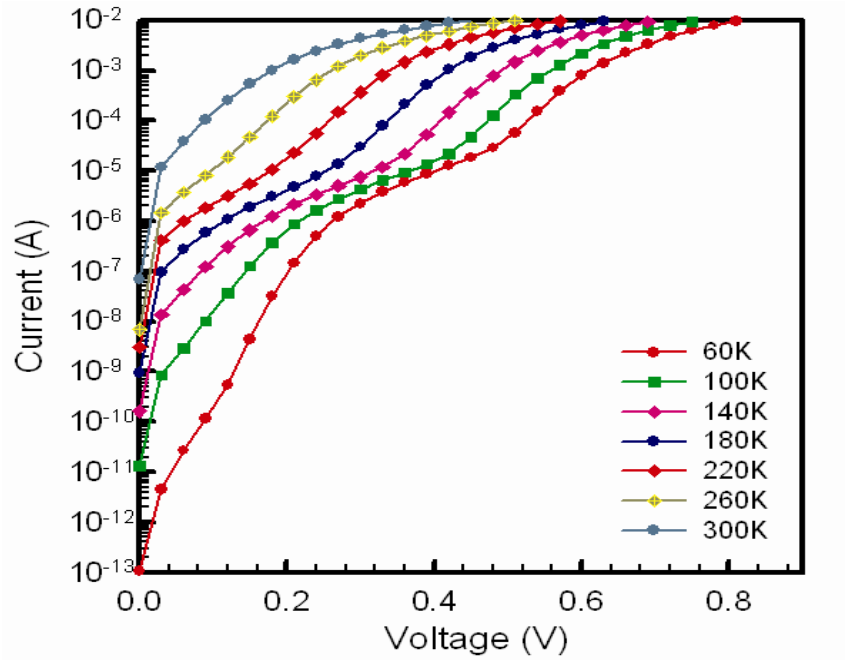

Fig. 8.2 *Experimental forward-bias current-voltage characteristics of a Pd/n-Ge (100) Schottky contact in the temperature range 60-300 K*

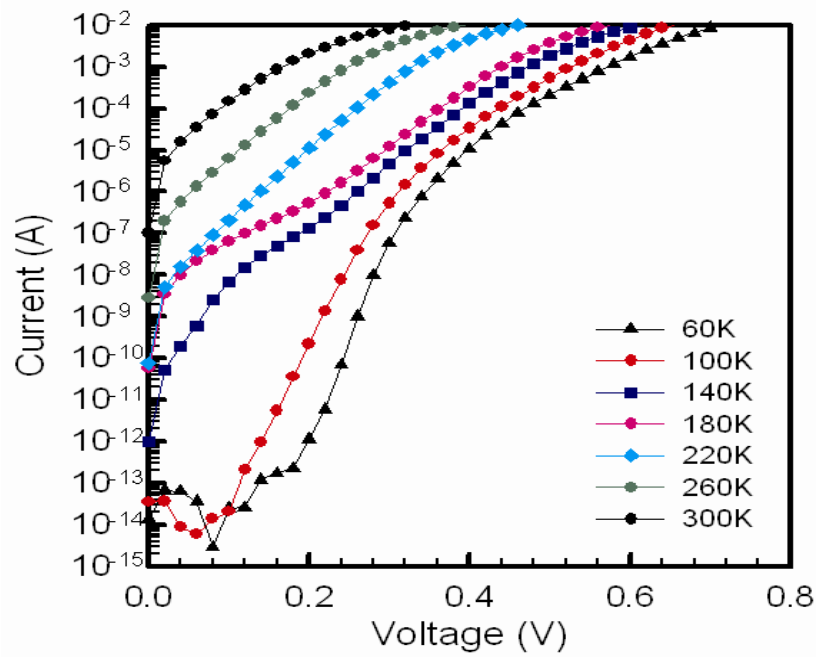

Fig. 8.3 *Experimental forward-bias current-voltage characteristics of a Au/n-Ge (100) Schottky contact in the temperature range 60-300 K*

Φ_B and n plots as a function of temperature for Ni-/, Pd-/ and Au/n-Ge (100) are presented in Figs. 8.4 – 8.6, respectively. The decrease in the barrier heights and increase in the ideality factors with decrease in temperature are observed from the *I-V* characteristics of Pd-/, Ni-/ and Au/n-Ge (100) Schottky contacts. This depicts that both parameters exhibit strong temperature dependence. This temperature dependence can be attributed to the discontinuities at the interface which may exist even for well controlled fabrication of the samples [34]. Since current transport across the MS interface is a temperature activated process, electrons at low temperatures are able to surmount the lower barriers [7], therefore, the current transport will be dominated by current flow through nanometer scale interfacial patches of small regions with lower SBH and larger ideality factors embedded in a higher background uniform barrier [31]. Because of these inhomogeneities, charge transport across the interface is no longer dominated by TE. Furthermore, many models have been evolved to explain the inhomogeneity in the barrier [31,35,36]. A potential fluctuation model was proposed by Tung [31] to explain the

inhomogeneity in BHs which show a larger deviation from the classical thermionic theory at low temperature.

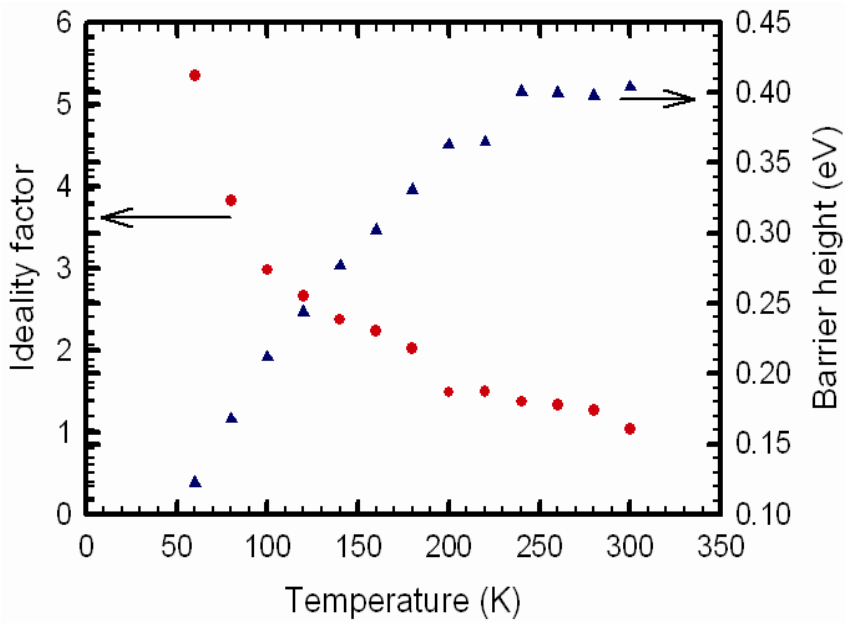

Fig. 8.4 *Temperature dependence of ideality factor and barrier height for Ni/n-Ge (100) Schottky contact in the temperature range 60-300 K*

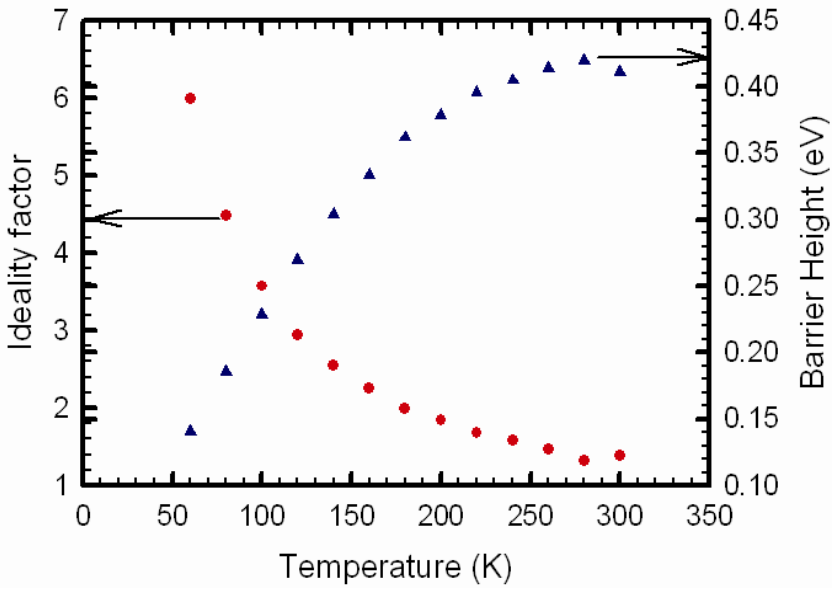

Fig. 8.5 *Temperature dependence of ideality factor and barrier height for Pd/n-Ge (100) Schottky contact in the temperature range 60-300* K

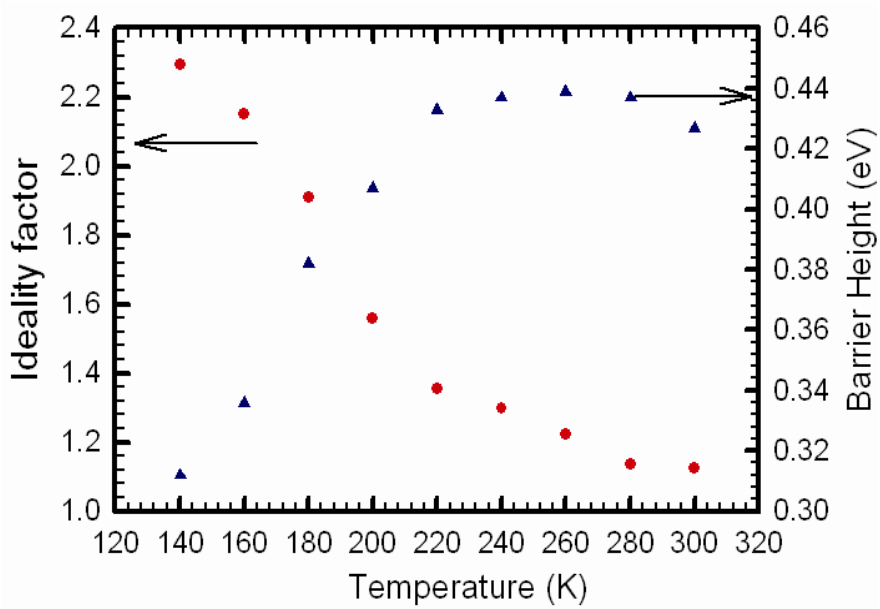

Fig. 8.6 *Temperature dependence of ideality factor and barrier height for Au/n-Ge (100) Schottky contact in the temperature range 140-300 K*

From the potential fluctuation model, at sufficiently low temperatures, a large number of patches may be present and consequently high current flowing through these patches. As the temperature increases, more electrons have sufficient energy to surmount the higher barrier [7,34]. As a result both the BH and ideality factor observed from temperature-dependent *I-V* characteristics (Figs. 8.4 – 8.6) are consistent with SBH inhomogeneity.

8.3.2 Analysis of inhomogeneous barrier height

The ideality factor is simply a manifestation of barrier uniformity [37]. BH inhomogenieties possibly originate from structural defects in semiconductors, inhomogeneous doping, interface roughness, interfacial reactions, diffusion/interdiffusion of the contaminants of deposited materials on semiconductor surfaces, inhomogeneities of thickness and composition of the layer, and non-uniformity of interfacial charges or the presence of a thin insulating layer between the metal and semiconductor [13,21,30,37,38,39]. The analysis of barrier height was also suggested and performed by Dokme et al. [40] and Karadeniz et al. [41]. The BH obtained under the flat

band condition is considered to be a real fundamental quantity which assumes that the electrical field is zero. This eliminates the effect of image force lowering that would affect the *I-V* characteristics and removes the influence of lateral inhomogeneity [40]. In order to describe the abnormal behaviours, i.e. the deviation from classical TE theory, a spatial distribution of the barrier height at the MS interface of Schottky contacts by a Gaussian distribution $P(\Phi_B)$ with a standard deviation (σ_s) around a mean SBH ($\bar{\Phi}_B$) value was suggested by Werner and Guttler [13,38] as:

$$P(\Phi_B) = \frac{1}{\sigma_s\sqrt{2\pi}} \exp\left[-\frac{(\Phi_B - \bar{\Phi}_B)^2}{2\sigma_s^2}\right], \tag{8.5}$$

where $\frac{1}{\sigma_s\sqrt{2\pi}}$ is the normalization constant of the Gaussian barrier distribution. The net current across a Schottky diode containing barrier inhomogeneities can be expressed as [40]

$$I(V) = \int_{-\infty}^{+\infty} I(\Phi_B, V) P(\Phi_B) d\Phi \ , \tag{8.6}$$

where $I(\Phi_B, V)$ is the current at a bias V for barrier height based on the ideal thermionic emission-diffusion (TED) theory and $P(\Phi_B)$ is the normalized distribution function giving the probability of accuracy for barrier height. The net current is then given by [40]

$$I(V) = I_s \exp\left(\frac{qV}{n_{ap}kT}\right)\left[1 - \exp\left(-\frac{qV}{kT}\right)\right], \tag{8.7}$$

with

$$I_s = A^* A T^2 \exp\left(-\frac{q\Phi_{ap}}{kT}\right), \tag{8.8}$$

where n_{ap} and Φ_{ap} are the experimental apparent ideality factor and apparent barrier height at zero bias, respectively, and given by [38]

$$\Phi_{ap} = \bar{\Phi}_B(T=0) - \frac{q\sigma_{s0}^2}{2kT} \tag{8.9}$$

$$\left(\frac{1}{n_{ap}} - 1\right) = -\rho_2 + \frac{q\rho_3}{2kT} \tag{8.10}$$

where ρ_2 and ρ_3 are the voltage coefficients that depict the voltage deformation of the barrier height distribution [37], while $\bar{\Phi}_B(T=0)$ and σ_{s0} are the mean barrier height and its standard deviation at the zero-bias ($V=0$), respectively.

The experimental Φ_B $vs\frac{1}{2kT}$ and $\left(\frac{1}{n}-1\right)vs\frac{1}{2kT}$ plots obtained by means of data from Figs. 8.1 – 8.3 for Pd-/, Ni-/ and Au/n-Ge (100) are shown in Figs. 8.7 – 8.9, respectively. The temperature dependence of the barrier height for Pd/n-Ge (100) Schottky diode (Fig. 8.7) depicts two Gaussian distributions with $\bar{\Phi}_{B1}(T=0)$ = 0.526 eV and σ_{s01} = 0.072 eV in 100 – 300 K and $\bar{\Phi}_{B2}(T=0)$ = 0.354 eV and σ_{s01} = 0.047 eV in 60 – 100 K.

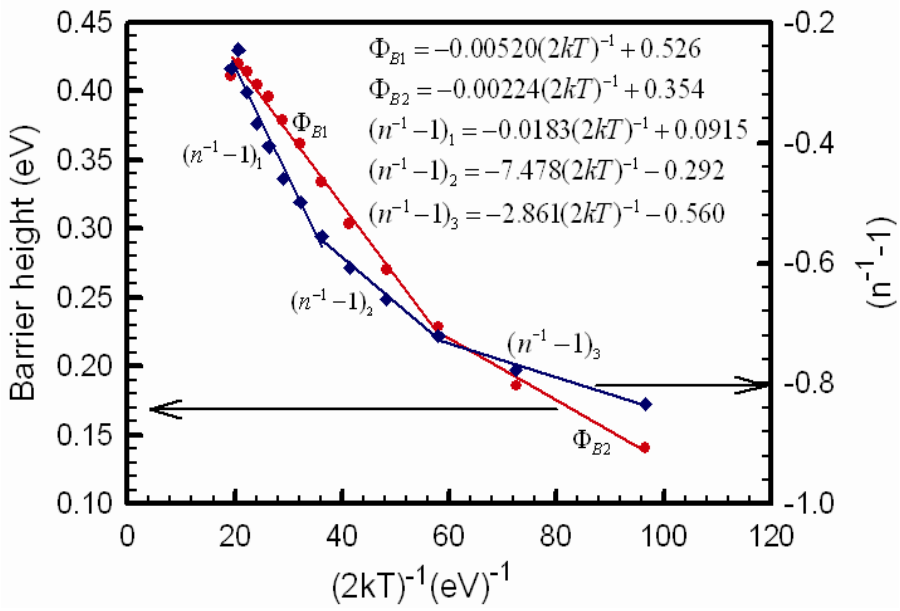

Fig. 8.7 *Temperature dependence of barrier height (Φ_B) and ideality factor (1/n −1) for Pd/n-Ge (100) Schottky diode.*

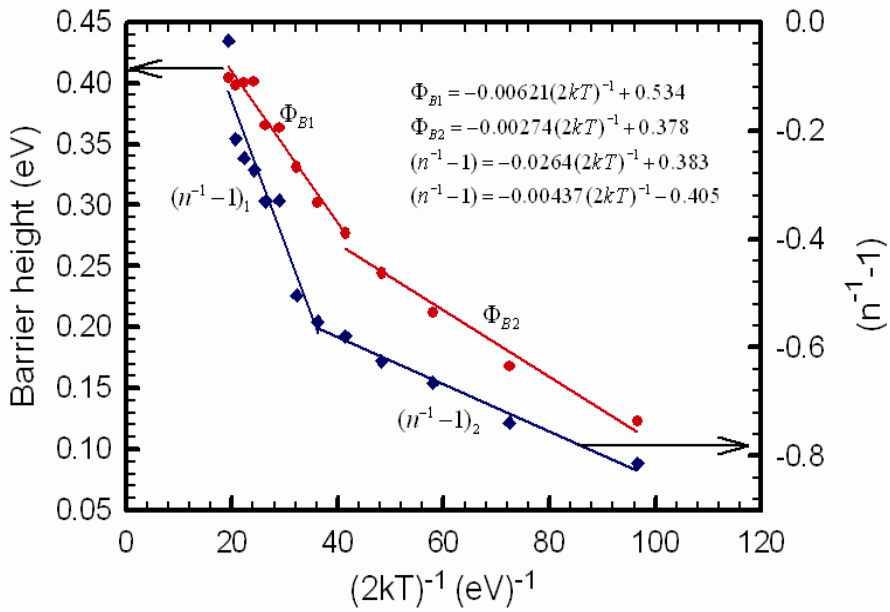

Fig. 8.8 *Temperature dependence of barrier height (Φ_B) and ideality factor (1/n −1) for Ni/n-Ge (100) Schottky diode.*

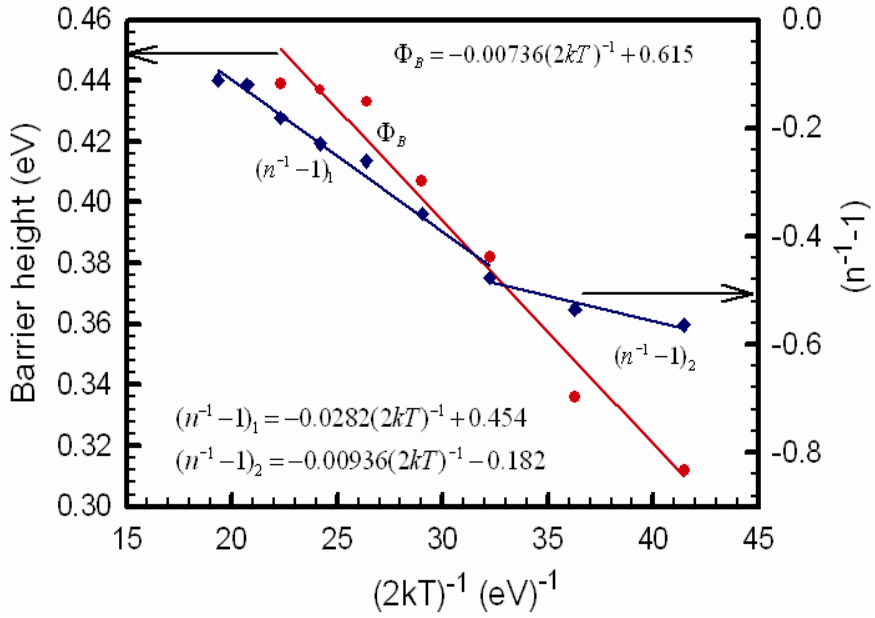

Fig. 8.9 *Temperature dependence of barrier height (Φ_B) and ideality factor (1/n −1) for Au/n-Ge (100) Schottky diode.*

The ideality factor for Pd/n-Ge (100) Schottky diode (Fig. 8.7) varies linearly with temperature in three distinct regions. The voltage coefficients have been obtained as $\rho_{21} = -0.0915$ and $\rho_{31} = -0.0183$ in 160 – 300 K range, $\rho_{22} = 0.292$ and $\rho_{32} = -7.478$ in 100 – 160 K range and $\rho_{23} = 0.560$ and $\rho_{33} = -2.861$ in 60 – 100 K range.

Fig. 8.8 shows a linear variation of barrier height and the ideality factor for Ni/n-Ge (100) Schottky contact. The data has been fitted to two regions whose Gaussian distribution parameters $\bar{\Phi}_B(T=0)$, σ_{s0} ρ_2 and ρ_3 have been extracted as $\bar{\Phi}_{B1}(T=0) = 0.534$ eV, $\sigma_{s01} = 0.0788$ eV, $\rho_{21} = -0.383$ and $\rho_{31} = -0.0264$ in 140-300 K range, and $\bar{\Phi}_{B2}(T=0) = 0.378$ eV, $\sigma_{s02} = 0.0523$ eV, $\rho_{22} = 0.405$ and $\rho_{32} = -0.0437$ in 60-140 K range.

The barrier height obtained from Au/n-Ge (100) Schottky diode is shown in Fig. 8.9. Parameters obtained for the Gaussian fit have been obtained as $\bar{\Phi}_{B1}(T=0) = 0.615$ eV and $\sigma_{s01} = 0.0858$ eV in 140-300 K. The data has been fitted to a single region. In this temperature range, the ideality factor shows some linearity with temperature in two regions. The voltage coefficients have been obtained as $\rho_{21} = -0.454$, and $\rho_{31} = -0.0282$ in 180-300 K range, $\rho_{22} = 0.182$ and $\rho_{32} = -0.00936$ in 140-180 K range.

When comparing $\bar{\Phi}_B(T=0)$ and σ_{s0} parameters, it is seen that the standard deviation is ≈ (13-15) % of the mean zero-bias barrier height. The standard deviation is a measure of barrier homogeneity. The lower value of σ_{s0} corresponds to a more homogeneous barrier height. These values of σ_{s0} are not small compared to their respective $\bar{\Phi}_B(T=0)$ and this indicates larger inhomogenieties at interface of Pd-/, Ni-/ and Au/n-Ge (100) structures. Hence, this inhomogeneity and potential fluctuations affect low temperature *I-V* characteristics. The linear behaviour of the plot from Eq. 8.10 demonstrates that the ideality factor does indeed express the voltage deformation of the Gaussian distribution of the SBH.

To determine the barrier height in another way, Eq. 8.2 can be rewritten as

$$\ln\left(\frac{I_0}{T^2}\right) = \ln(AA^*) - \frac{q\Phi_{B0}}{kT} \tag{8.11}$$

The Richardson constant is usually determined from the intercept of $\ln\left(\frac{I_0}{T^2}\right) versus \frac{1000}{T}$ plot. Figs 8.10-8.12 show the conventional energy variation of $\ln\left(\frac{I_0}{T^2}\right) versus \frac{1000}{T}$ (labelled y_1) for Pd-, Ni- and Au/n-Ge (100) Schottky diodes, respectively. The experimental data are shown to fit asymptotically to a straight line at higher temperatures. Since the conventional Richardson plot deviates from linearity at low temperatures due to the barrier inhomogeneity, it can be modified by combining Eq. 8.8 and 8.9 as follows

$$\ln\left(\frac{I_s}{T^2}\right) - \left(\frac{q^2\sigma_{s0}^2}{2k^2T^2}\right) = \ln\left(A^*A\right) - \frac{q\bar{\Phi}_{B0}}{kT} \tag{8.12}$$

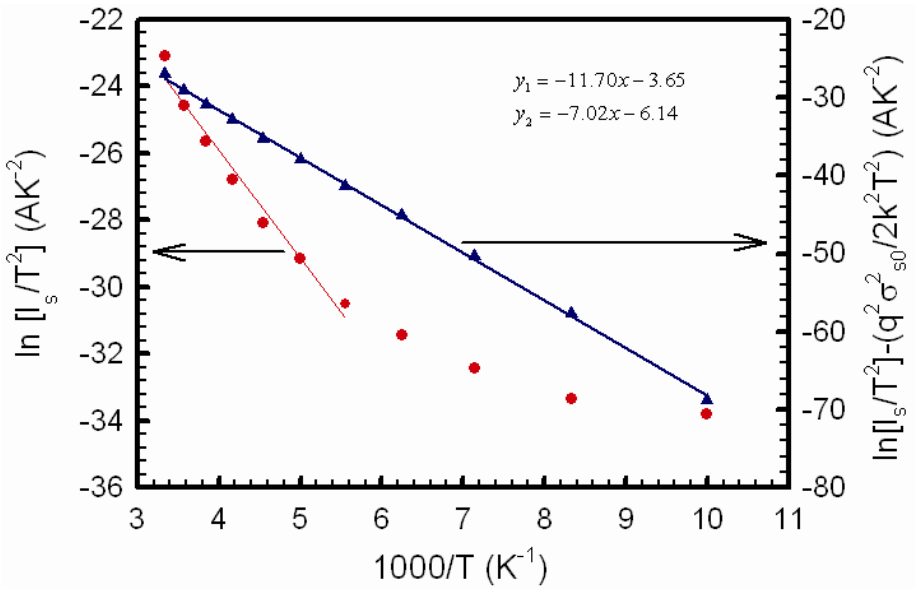

Fig. 8.10 *Richardson's plot of* $\ln\left(\frac{I_0}{T^2}\right) versus \frac{1000}{T}$ *and modified* $\ln\left(\frac{I_s}{T^2}\right) - \left(\frac{q^2\sigma_{s0}^2}{2k^2T^2}\right) versus \frac{1000}{T}$ *for Pd/n-Ge (100) Schottky diode.*

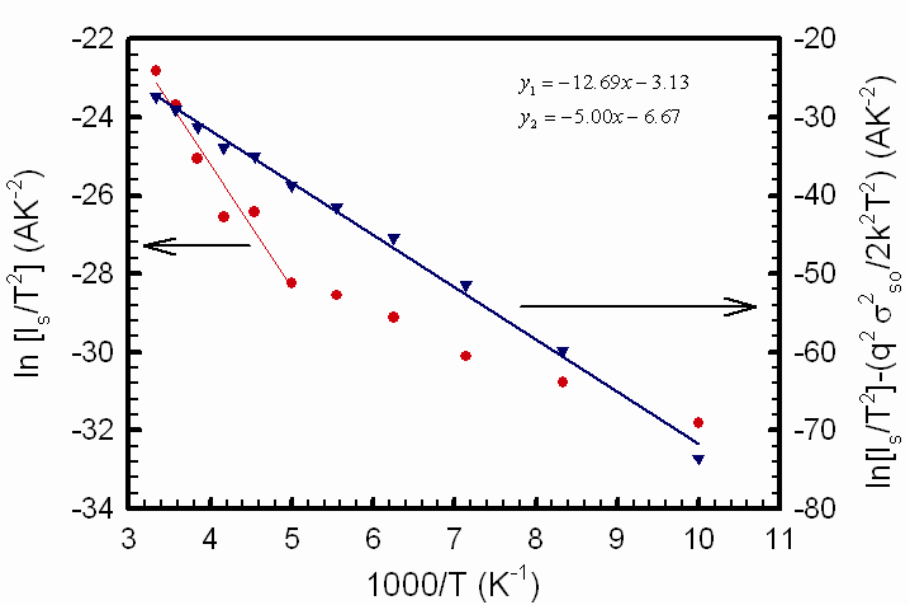

Fig. 8.11 *Richardson's plot of* $\ln\left(\frac{I_0}{T^2}\right)$ *versus* $\frac{1000}{T}$ *and modified* $\ln\left(\frac{I_s}{T^2}\right)-\left(\frac{q^2\sigma_{s0}^2}{2k^2T^2}\right)$ *versus* $\frac{1000}{T}$ *for Ni/n-Ge (100) Schottky diode.*

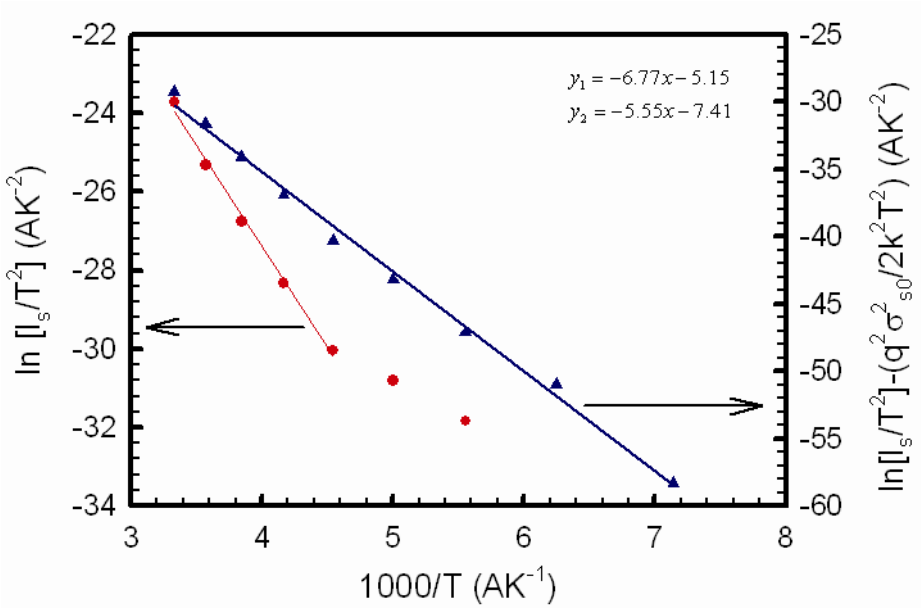

Fig. 8.12 *Richardson's plot of* $\ln\left(\frac{I_0}{T^2}\right)$ *versus* $\frac{1000}{T}$ *and modified* $\ln\left(\frac{I_s}{T^2}\right)-\left(\frac{q^2\sigma_{s0}^2}{2k^2T^2}\right)$ *versus* $\frac{1000}{T}$ *for Au/n-Ge (100) Schottky diode.*

Figs. 8.10-8.12 show the modified $\ln\left(\frac{I_s}{T^2}\right)-\left(\frac{q^2\sigma_{s0}^2}{2k^2T^2}\right) versus \frac{1000}{T}$ plot (labelled y_2) for Pd-/, Ni- and Au/n-Ge (100) Schottky diodes, respectively. The modified plot gives $\bar{\Phi}_B(T=0)=$ 0.529 eV and $A^*=$ 0.32 Acm^{-2}K^{-2} for Pd/n-Ge Schottky structures, $\bar{\Phi}_B(T=0)=$ 0.575 eV and $A^*=$ 2.38 Acm^{-2}K^{-2} for Ni/n-Ge Schottky structures and $\bar{\Phi}_B(T=0)=$ 0.639 eV and $A^*=$ 1.37 Acm^{-2}K^{-2} for Au/n-Ge Schottky structures. The values of $\bar{\Phi}_B(T=0)$ have almost the same values as the mean BHs obtained from the Φ_B *vs* $\frac{1}{2kT}$ plot at higher temperatures in Figs 8.7- 8.9. The modified Richardson constant from the modified plots ranges between 0.32 and 2.38 Acm^{-2}K^{-2}. Yao et al. [42] and Zhu et al. [43] have reported the n-type Ge Richardson constant to be 50 and 67 Acm^{-2}K^{-2}, respectively.

8.4 Summary and conclusions

The *I-V-T* characteristics of Pd-/, Ni-/ and Au/n-Ge (100) Schottky contacts fabricated using the resistive evaporation system were measured in the 40-300 K temperature range. The ideality factors were seen to increase while barrier heights decrease with decreasing temperature. These observations have been attributed to barrier inhomogeneities at the MS interface. The *I-V* characteristics of these Schottky contacts over a wide temperature range have been successfully modelled on the basis of the TE mechanism by assuming the presence of multiple Gaussian distributions of barrier heights in the 40-300 K temperature range. Chand and Kumar [44] have indicated that the existence of multiple Gaussian distributions in MS contacts can be attributed to the nature of the inhomogenieties themselves. This may involve variation in interface composition/phase, interface quality, electrical charges and non-stoichiometry, etc [45].

References

[1] E.H. Rhoderick, R.H. Williams, Metal-Semiconductor Contacts, Clarendon Press, Oxford University Press, Oxford, 1988.

[2] H. Cetin, E. Ayyildiz, Semicond. Sci. Technol. **20** (2005) 625.

[3] R.L. Van Meirhaeghe, W.H. Laflére, F. Cardon, J. Appl. Phys. **76** (1994) 403.

[4] E. Gur, S. Tuzemen, B. Kilic, C. Coskun, J. Phys. Condens. Matter. **19** (2007) 1966206.

[5] N. Rouag, L. Boussouar, S. Toumi, Z. Ounnoughi, M.A. Djouadi, Semicond. Sci. Technol. **22** (2007) 369.

[6] D.M. Kim, D.H. Kim, S.Y. Lee, Solid-State Electron. **51** (2007) 865.

[7] F.E. Cimilli, M. Sağlam, H. Efeoğlu, A. Türüt, Physica B **404** (2009) 1558.

[8] S.M. Sze, Physics of Semiconductor Contacts, 2nd .ed., Wiley, New York, 1981.

[9] R.T. Tung, Mater. Sci. Eng. R **35** (2001) 1.

[10] Dhananjay, J. Nagaraju, S.B. Krupanidhi, Physica B **391** (2007) 344.

[11] A.R. Arehart, B. Moran, J.S. Speck, U.K. Mishra, S.P. Den Baars, S.A. Ringel, J. Appl. Phys. **100** (2006) 023709.

[12] A.F. Qasrawi, Semicond. Sci. Technol. **21** (2006) 794).

[13] J.H. Werner, H.H. Guttler, J. Appl. Phys. **73** (1993) 1315.

[14] S. Chattopadhyay, L.K. Bera, S.K. Ray, K. Maiti, Appl. Phys. Lett. **71** (1997) 942.

[15] T.P. Chen, T.C. Lee, C.C. Ling, C.D. Beling, S. Fung, Solid-State Electron. **36** (1993)

949.

[16] M.K. Hudait, P. Venkatesvarlu, S.B. Krupanidhi, Solid-State Electron. **45** (2001) 133.

[17] Ş. Karataş, Ş. Altindal, A. Türüt, A. Özmen, Appl. Surf. Sci. **217** (2003) 250.

[18] T. Sawada, Y. Ito, N. Kimura, K. Imai, K. Suzuki, S. Sakai, Appl. Surf. Sci. **190** (2002) 326.

[19] J. Osvald, Zs.J. Horváth, Appl. Surf. Sci. **234** (2004) 349.

[20] N. Tuğluoğlu, S. Karadeniz, M. Şahin, H. Şafak, Appl. Surf. Sci. **233** (2004) 320.

[21] M. Soylu, B. Abay, Microelectron. Eng. **86** (2009) 88.

[22] W. Mtangi, F.D. Auret, C. Nyamhere, P.J. Janse van Rensburg, M. Diale, A. Chawanda, Physica B **404** (2009) 1092.

[23] F.E. Cimilli, M. Sağlam, H. Efeoğlu, A. Türüt, Physica B **404** (2009) 1558.

[24] Ö. Faruk Yüksel, Physica B **404** (2009) 1993.

[25] M. Pattabi, S. Krishnan, Ganesh, X. Mathew, Solar Energy **81** (2007) 111.

[26] F. Brovelli, B.L. Rivas, J.C. Bernede, J. Chilean, Chem Soc. **52** (2007) 1065.

[27] F. Yakuphanoglu, Physica B **389** (2007) 306.

[28] H.J. Im, Y. Ding, J.P. Pelz, W.J. Choyke, Phys. Rev. B **64** (2001) 075310.

[29] R.F. Schmitsdorf, T.U. Kampen, W. Mönch, J. Vac Sci. Technol. B **15** (1997) 1221.

[30] J.P. Sullivan, R.T. Tung, M.R. Pinto, W.R. Graham, J. Appl. Phys **70** (1991) 7403.

[31] R.T. Tung, Phys. Rev. B **45** (1992) 13509.

[32] W.P. Leroy, K. Opsomer, S. Forment, R.L. Van Meirhaeghe, Solid-State Electron. **49** (2005) 878.

[33] F.E. Cimilli, M. Saglam, A. Turut, Semicond. Sci. Technol. **22** (2007) 851.

[34] M.B. Reddy, A.A. Kumar, V. Janardhanam, V. R. Reddy, P.N. Reddy, Current. Appl. Phys. **9** (2009) 972.

[35] J.D. Levine,J. Appl. Phys. **42** (1971) 3991.

[36] F.A. Padovani, R. Stratton, Solid-State Electron. **9** (1996) 695.

[37] S. Zhu, R.L. Van Meirhaeghe, S. Forment, G.P. Ru, X.P. Qu, B.Z. Li, Solid State Electron. **48** (2004) 1205.

[38] J.H. Werner, H.H. Guttler, J. Appl. Phys. **69** (1991) 1522.

[39] Y.P. Song, R.L. Van Merhaeghe, W.H. Laflare, F. Cardon, Solid State Electron. **29** (1986) 633.

[40] I. Dokme, S. Altindal, M.M. Bulbul, Appl. Surf. Sci. **252** (2006) 7749.

[41] Ş. Karadeniz, M. Şahim, N. Touğluoğlu, H. Şafak, Semicond. Sci. Technol. **19** (2004) 1098.

[42] H.B. Yao, C.C. Tan, S.L. Liew, C.T. Chua, C.K. Chua, R. Li, R.T.P. Lee, S.J. Lee, D.Z. Chi, International Workshop on Junction Technology Proc (2006) 164.

[43] S. Zhu, A. Nakajima, Y. Yokoyama and K. Ohkura, International Workshop on Junction Technology Proc (2005) 85.

[44] S. Chand, J. Kumar, Semicond. Sci. Technol. **11** (1996) 1203.

[45] S. Doğan, S. Duman, B. Gürbuolak, S. Tüzemen, H. Morkoç, Physica E **41** (2009) 64.

CHAPTER 9

Conclusions

Conclusions specific to each of the experimental results are presented at the end of every chapter. In this chapter a brief summary of the results is presented.

Thermal annealing behaviour of metal Schottky contacts on n-Ge (100)

The Schottky contact behaviour was investigated under various furnace annealing conditions. The variation of Schottky barrier heights and ideality factors with annealing temperature may be attributed to interfacial reactions of the metals with germanium and phase transformation of metal-germanides during annealing. The as-deposited barrier heights near the bandgap of Ge in Pt/-, Ni/-, Ti/- and Ir/n-Ge (100) Schottky contacts imply that these metals form good Schottky source/drain contacts in p-channel Ge-MOSFETs, for hole injection from source into inverted p-channel. The results also show that Pt/n-Ge (100) and Ru/n-Ge (100) Schottky contacts are highly thermally stable over a wide range of temperature, 25 – 600°C and 25 – 550°C, respectively.

Morphological evolution of metal Schottky contacts on n-Ge (100)

SEM observations were conducted for samples annealed at different temperatures. From the SEM images, it can be concluded that the onset temperature for agglomeration in 30 nm Ni/n-Ge (100), and Pt/-, Ir/- and Ru/n-Ge (100) systems occur at 500 – 600°C and 600 – 700°C, respectively. Grain growth at the surface of these metals was evident up to 500°C, suggesting a better morphological stability.

The barrier height distribution in identically prepared Schottky contacts on n-Ge (100)

The barrier heights and the ideality factors were obtained from the individual *I-V* characteristics of the MS contacts. It has been shown that the barrier heights and the ideality factors varied from diode to diode even though they were identically fabricated. The homogeneous barrier height values were obtained for the metals on n-Ge Schottky contacts from the linear relationship between the *I-V* effective barrier heights and ideality factors, which can be explained by lateral

inhomogeneities. The agreement between experimental data and theoretical predictions on Pd/n-Ge (100), Ni/n-Ge (100) and Au/n-Ge (100) contacts were an interesting experimental illustration of the theoretical predictions [1,2,3].

Studies of defects induced in Sb doped Ge during contacts fabrication and the annealing process.

DLTS and L-DLTS have been successfully used to characterize the defects induced in n-Ge during metallization by electron beam deposition and subsequent annealing processes. These techniques have revealed that the dominant defect induced by electron beam deposition is the V-Sb (*E*-centre) complex. The source of the damage has been due to the residual vacuum gases, which were ionized around the filament and then accelerated by the electric and magnetic field towards the substrate, introducing vacancy-interstitial pairs beneath the semiconductor surface, which are mobile and form stable mainly vacancy-related defects. All defects induced during electron beam deposition and annealing were removed from Ge with very low thermal budget of between 200-350°C. This indicates low binding energies of defects in Ge.

Current-Voltage Temperature characteristics of n-Ge (100) Schottky barrier diodes.

The n-Ge Schottky contacts have revealed a strong dependence on temperature. The current transport mechanism has been shown to be predominantly thermionic emission at high temperatures (i.e. close to room temperature) while at low temperatures, the Schottky contacts have exhibited the dominance of the generation-recombination current mechanism. From the *I-V* measurements, the ideality factors were seen to increase and barrier heights decrease with decreasing temperature. This have been attributed to the presence of a wide distribution of low SBH patches at the metal-germanium interface, leading to the flow of excess current at low voltages and temperatures.

Future Work

Further studies need to be carried out to investigate the following:

(i) Identification of the composition of residual vacuum particles during electron beam metallization process.

(ii) The effects of a metal shield in the EB system to protect the Ge sample from energetic particles originating at the filament during the electron beam deposition, on the electrical properties of Ge Schottky contacts.

(iii) Structural characterization of metal germanides using XRD, XPS, AES and Raman spectroscopy techniques.

(iv) Establishment of defect concentration profile, annealing mechanisms for prolonged time: model.

References

[1] R.T. Tung, Phys. Rev. B **45** (1992) 13509.

[2] J.P. Sullivan, R.T. Tung, M.R. Pinto, W.R. Graham, J. Appl. Phys. **70** (1991) 7403.

[3] R.F. Schmitsdorf, T.U. Kampen, W. Mönch, **15** (1997) 1221.